



Derivation of the Probability Density Functions for the Local Joint Flexibility Factors in Axially Loaded Two-Planar Tubular DK-Joints of Offshore Structures

Hamid Ahmadi ^{a,*}, Vahid Mayeli ^b

^a Faculty of Civil Engineering, University of Tabriz, Tabriz 5166616471, Iran

Center of Excellence in Hydroinformatics, Faculty of Civil Engineering, University of Tabriz, Tabriz, Iran

^b Faculty of Civil Engineering, University of Tabriz, Tabriz 5166616471, Iran

Received 11 May 2019; Accepted 17 August 2020

ABSTRACT:

Probability density functions of the involved random variables are essential for the reliability-based design of offshore structures. The objective of present research was the derivation of probability density function (PDF) for the local joint flexibility (LJF) factor, f_{LJF} , in two-planar tubular DK-joints commonly found in jacket-type offshore structures. A total of 162 finite element (FE) analyses were carried out on 81 FE models of DK-joints subjected to two types of axial loading. Generated FE models were validated using available experimental data, FE results, and design formulas. Based on the results of parametric FE study, a sample database was prepared for the f_{LJF} values and density histograms were generated for respective samples based on the Freedman-Diaconis rule. Nine theoretical PDFs were fitted to the developed histograms and the maximum likelihood (ML) method was applied to evaluate the parameters of fitted PDFs. In each case, the Kolmogorov-Smirnov and chi-squared tests were used to evaluate the goodness of fit. Finally, the Inverse Gaussian model was proposed as the governing probability distribution function for the f_{LJF} . After substituting the values of estimated parameters, two fully defined PDFs were presented for the f_{LJF} in tubular DK-joints subjected to two types of axial loading.

KEYWORDS:

Tubular DK-joint, LJF factor, Probability density function (PDF), Inverse Gaussian model, Goodness-of-fit test.

1. Introduction

A jacket that is a welded steel space frame fabricated with circular hollows section (CHS) members is one of the most frequently used structural systems for the substructure of offshore wind turbines (OWTs) and oil/gas production platforms in shallow and intermediate water depths. The connection of the CHS members in which the prepared ends of brace members are welded onto the undisturbed surface of a chord member is called a tubular joint (Fig. 1a).

One of the factors affecting the global static and dynamic responses of an offshore structure is the local joint flexibility (LJF) which is an intrinsic feature of a tubular joint. The LJF increases the

deflections, redistributes the nominal stresses, reduces the buckling loads and changes the natural frequencies of the structure (Bouwkamp et al., 1980; Underwater Engineering Group (UEG), 1985; Gao et al., 2013). For example, analysis of a jacket platform considering the local flexibility of the joints results in higher primary natural period of vibration and lower base shear compared to the case in which the joints are assumed to be rigid. These facts imply that the conventional procedures for the analysis and design of tubular structures with the assumption that the tubular joints are rigid may not be accurate enough, especially for unstiffened joints. Hence, it is necessary to determine the local joint flexibility for commonly used tubular joints.

The primary factors that affect the LJF are the joint type, its geometrical properties, and brace loading type. In order to relate the behavior of a

* Corresponding Author

E-mail addresses: h-ahmadi@tabrizu.ac.ir (Hamid Ahmadi); mayeli.vahid@gmail.com (Vahid Mayeli).

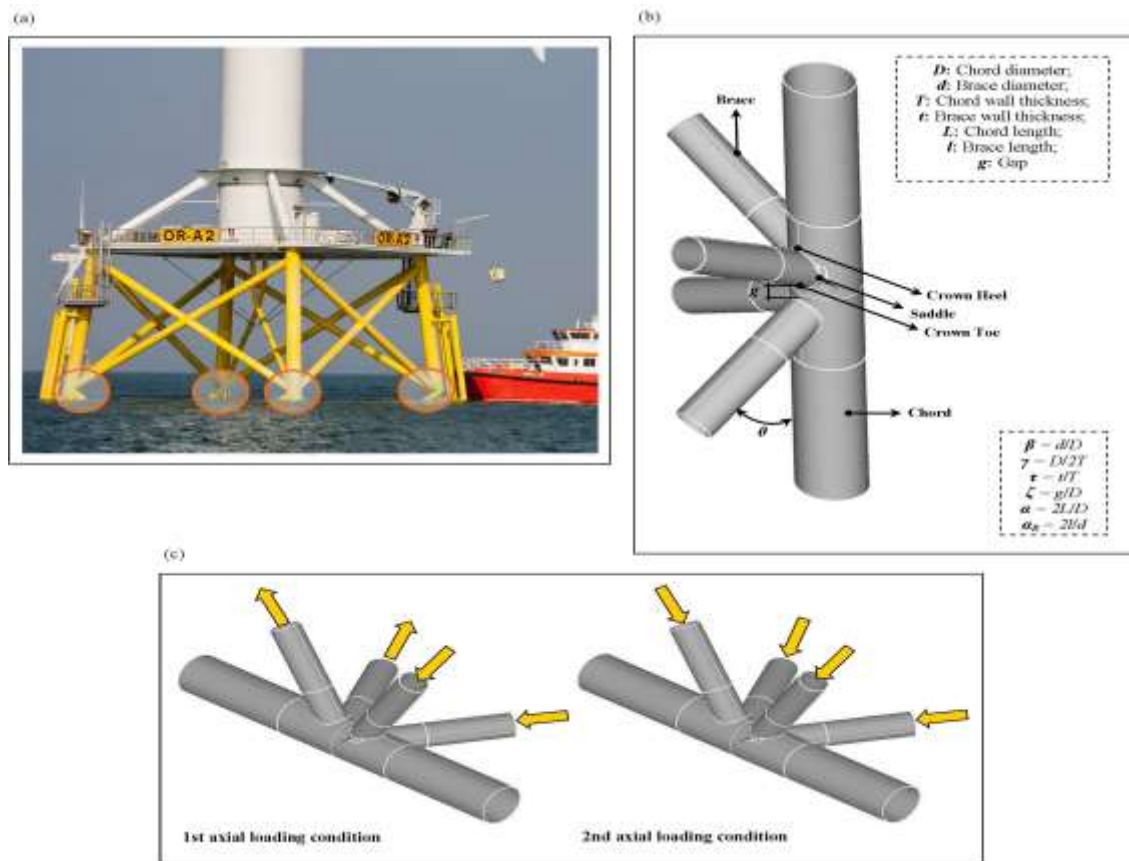


Fig. 1. (a) Two-planar tubular DK-joints in an OWT jacket substructure, (b) Geometrical notation for a two-planar DK-joint, (c) Considered axial loading conditions

tubular joint to its geometrical characteristics, a set of dimensionless geometrical parameters including α , α_B , β , γ , τ , and ζ , defined in Fig. 1b, is commonly used.

Static and dynamic analyses of deterministic type usually lead to conservative designs. The reason is that in a deterministic analysis, limiting assumptions should be made on numerous input parameters some of which exhibit considerable scatter. This fact emphasizes the significance of reliability-based analysis and design methods in which the key parameters of the problem can be modeled as random variables. The fundamentals of reliability assessment, if properly applied, can provide immense insight into the performance and safety of the structural system. Regardless of the method used for the reliability-based analysis and design of steel offshore structures, the probabilistic and statistical measures of the LJF are required as input parameters. The LJF shows considerable scatter highlighting the significance of deriving its governing probability distribution function.

In the present research, a total of 162 finite element (FE) analyses were carried out on 81 FE models of two-planar tubular DK-joints which are among the most common joint types in jacket substructure of OWTs and oil/gas production platforms. FE analyses were conducted under two types of axial loading as shown in Fig. 1c. Generated

FE models were validated using the existing experimental data, FE results, and design formulas. Based on a parametric FE investigation, a sample database was created for the LJF factor (f_{LJF}) (Sect. 3); and density histograms were generated for respective samples based on the Freedman-Diaconis rule (Sect. 4). Nine theoretical probability density functions (PDFs) were fitted to the developed histograms and the maximum likelihood (ML) method was applied to evaluate the parameters of fitted PDFs (Sect. 5). In each case, the Kolmogorov-Smirnov and chi-squared tests were used to assess the goodness of fit (Sect. 6). Finally, a probability distribution model was proposed for the f_{LJF} ; and after substituting the values of estimated parameters, two fully defined PDFs were presented for the f_{LJF} in two-planar tubular DK-joints under two types of axial loading (Sect. 7).

2. Literature survey

Underwater Engineering Group, UEG (1985) and Det Norske Veritas, DNV (1977) have provided parametric equations to determine the LJF for tubular T-/Y-joints. The UEG guidelines do not clearly define the range of applicability; and the DNV equations are based on a limited number of FE analyses. Efthymiou (1985) developed a set of equations for T-, Y-, and K-joints subjected to in-

plane bending (IPB) and out-of-plane bending (OPB) loads by numerical analysis. The database was limited to 12 T-, 3 Y-, and 5 K-joints, 5 of which were partially overlapped.

Fessler et al. (1986) measured the local deformation of the chord wall subjected to basic loadings within the elastic range based on 27 models and derived a set of parametric equations for both T-/Y- and K-joints. However, their experimental models were made from araldite instead of steel; and they had relatively small scale. Ueda et al. (1990) proposed a set of equations to predict the LJF under the axial and IPB loads based on FE analysis of 11 T-joint models. The results amended and improved the accuracy and maintained the simplicity of numerical computation as well. However, the validity range of geometrical parameters for these equations was very limited in terms of brace-to-chord diameter ratio, which was restricted to 0.35–0.55.

Chen et al. (1990) determined the LJF of T-, Y-, and K-joints. By using the semi-analytical approach, Chen et al. (1993) and Hoshyari and Kohoutek (1993) quantified the LJF for simple gap K- and T-/Y-joints, respectively. Buitrago et al. (1993) provided the methodology as well as the parametric equations for computing the LJF in gap and partially overlapped joints based on the FE analysis. Chen and Zhang (1996) studied the stress distribution in space frames with the consideration of local flexibility of multi-planar tubular joints.

Hu et al. (1993) and Golafshani et al. (2013) proposed equivalent elements representing the local flexibility of tubular joints in structural analysis of offshore platforms. Gao et al. (2013, 2014) and Gao and Hu (2015) proposed parametric equations to predict the LJF in completely overlapped tubular joints subjected to axial, IPB, and OPB loadings, respectively.

Ahmadi and Ziaei Nejad (2017) developed a set of parametric equations to determine the LJF in two-planar tubular DK-joints subjected to axial, IPB, and OPB loadings, respectively. They indicated that the effect of multi-planarity on the LJF can be significant and consequently the use of the equations already available for uniplanar joints to calculate the LJF in multi-planar joints may lead to highly under-/over-predicting results. Their finding was in agreement with previous studies suggesting that the stress and strain distribution in multi-planar tubular joints might be quite different from the uniplanar ones (Karamanos et al., 1999; Ahmadi et al., 2011; Ahmadi and Lotfollahi-Yaghin, 2012; Ahmadi and Zavvar, 2016).

Ahmadi and Mayeli (2018, 2019) developed a set of probability distribution models for the LJF factors in offshore two-planar tubular DK-joints subjected to IPB and OPB moment loadings.

For other investigations related to tubular joints such as the studies on the stress concentration factor (SCF), degree of bending (DoB), and static

strength, the reader is referred for example to (Ahmadi et al., 2011; Ahmadi et al., 2019; Nassiraei et al., 2016, 2017, 2018, 2019; Nassiraei, 2019), among many others.

The above discussion on the previous investigations of the LJF indicates that the LJF for uniplanar tubular joints such as T-/Y-, X-, and K-joints due to basic load cases has been extensively studied; based on which a set of parametric equations have been derived. However, for multi-planar tubular joints which cover the majority of practical applications, the research works in terms of the LJF are very limited mainly due to the more complexities involved in modeling. Moreover, results of research works reported in the literature are suitable for deterministic analyses. To the best of the authors' knowledge, no probabilistic study has been carried out on the LJF; and there is no probability density function available for the LJF factors to be used in reliability-based static and dynamic analyses.

3. Preparation of the f_{LJF} samples

3.1. Determination of the f_{LJF} under the axial loading

The LJF of an axially loaded tubular joint is defined as the displacement attributed to the local chord wall deformation due to a unit applied load. It measures the distortion of the CHS which is an oval shape under the axial loading without considering the beam bending movement (Gao et al., 2013).

The LJF of a tubular joint under the axial loading can be calculated as follows:

$$LJF = (\delta_{AX} / P_{AX}) \sin \theta \quad (1)$$

where θ is the brace inclination angle (Fig. 1b), P_{AX} is the axial load of the brace, and δ_{AX} is the displacement caused only by chord wall deformation, in which overall bending deflection of the chord acting as a beam must be excluded.

Since the intersection of the brace and chord members is a space curve, for the purpose of actual calculation in an FE model, δ_{AX} can be expressed as the average local displacement of the joint normal to the chord axis:

$$\delta_{AX} = \frac{(\delta_1 - \delta'_1) + (\delta_2 - \delta'_2) + (\delta_3 - \delta'_3) + (\delta_4 - \delta'_4)}{4} \quad (2)$$

where δ_1 , δ_2 , δ_3 , and δ_4 are the displacements at the crown toe, crown heel, and two saddle positions measured perpendicular to the chord axis; and δ'_1 , δ'_2 , δ'_3 , and δ'_4 are the bending deflections that can be determined by simple beam theory. Saddle, crown toe, and crown heel positions are shown in Fig. 1b.

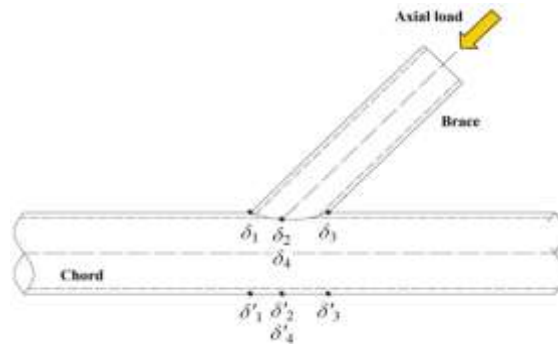


Fig. 2. Positions for the deformation measurement to determine the f_{LJF} in a tubular joint under the axial loading

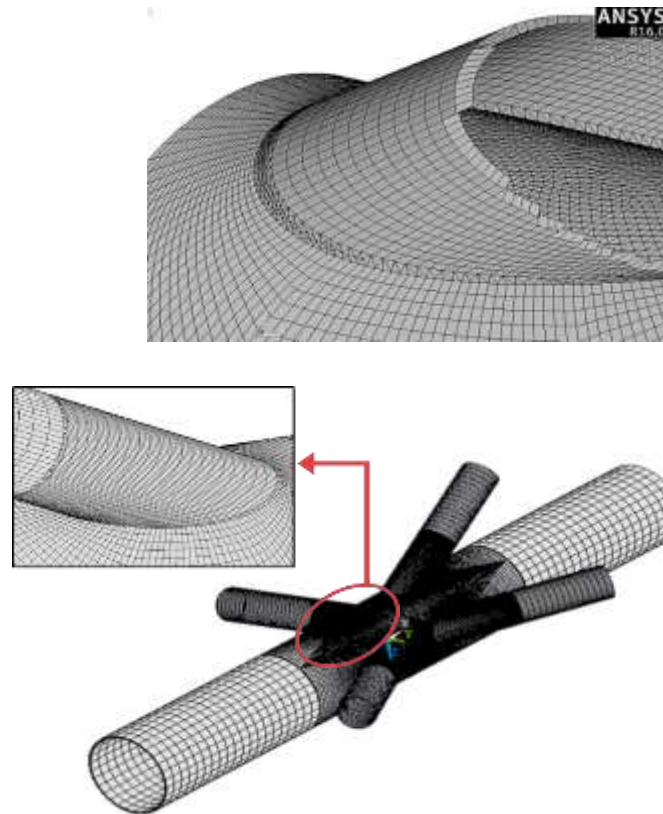


Fig. 3. The mesh generated for a two-planar tubular DK-joint using the sub-zone method

According to Gao et al. (2013, 2014), bending deflections in a FE model can be reasonably approximated by the displacements at the bottom of the chord member corresponding to δ_1 , δ_2 , δ_3 , and δ_4 , respectively (Fig. 2). The reader is referred to Chen et al. (1990) for the details of deriving Eqs. (1) and (2).

In order to relate the local joint flexibility to dimensionless geometrical parameters of the joint, a dimensionless coefficient called the local joint flexibility parameter (f_{LJF}) is defined. Under the axial loading, the f_{LJF} is the LJF multiplied by ED :

$$f_{LJF} = (\delta_{AX} / P_{AX}) ED \sin \theta \quad (3)$$

where D is the chord diameter and E is the Young's modulus.

Since a two-planar DK-joint has four brace members, there are four different positions for the application of (1)–(3). However, due to the symmetry in the geometry of the joint and either symmetry or antisymmetry in the applied loading, results obtained from all of these four positions would be the same.

3.2. FE modeling procedure

3.2.1. Modeling of the weld profile

The welding size along the brace-to-chord intersection satisfies the AWS D 1.1 (2002) specifications. Details of the weld profile modeling according to AWS D 1.1 (2002) are presented and discussed by Ahmadi et al. (2012).

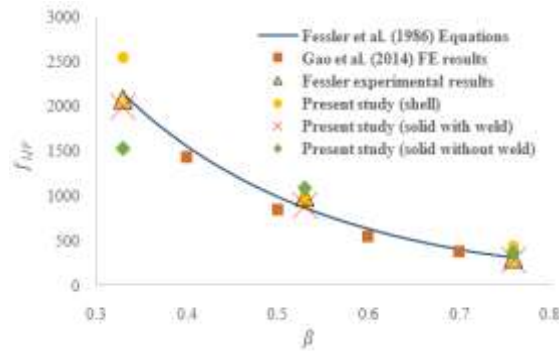


Fig. 4. Results of the FE model validation

Table 1. Geometrical properties of validating Y-joint models

Geometrical parameter	Value	Dimensionless parameters
Chord length	$L = 1888.0$ mm	
Chord diameter	$D = 168.3$ mm	$\alpha = 2L/D = 22.4$
Chord wall thickness	$T = 7.0$ mm	$\gamma = D/2T = 12$
Brace length	$l = 623.0$ mm	$\beta = d/D = 0.32, 0.53, 0.76$
Brace diameter	$d = 55.5, 88.2, 127.9$ mm	$\tau = t/T = 0.78$
Brace wall thickness	$t = 5.5$ mm	
Brace inclination angle	$\theta = 60^\circ$	

Table 2. Comparing the results of validating FE model and the experimental data

β	f_{LJF}				Error (%)		
	Validating FE model			Experimental data [6]	Shell	Solid with weld	Solid without weld
	Shell	Solid with weld	Solid without weld				
0.32	2538.45	1996.40	1525.39	2079.33	22.08	4.15	36.31
0.53	954.39	895.39	1083.61	985.57	3.16	10.07	9.94
0.76	437.98	277.63	360.95	300.48	45.75	8.22	20.12

Table 3. Comparing the results of validating FE model and the equation proposed by Fessler et al. (1986)

β	f_{LJF}			Fessler et al. (1986) equation	Error (%)		
	Validating FE model				Shell	Solid with weld	Solid without weld
	Shell	Solid with weld	Solid without weld				
0.32	2538.45	1996.40	1525.39	2133.41	18.98	6.86	39.86
0.53	954.39	895.39	1083.61	877.40	8.77	2.05	23.50
0.76	437.98	277.63	360.95	312.50	40.15	12.00	15.50

Table 4. Statistical measures of the generated f_{LJF} samples

Statistical measure	f_{LJF} samples	
	Sample 1 (1 st axial load case)	Sample 2 (2 nd axial load case)
n	81	81
μ	21.1588	20.8825
σ	17.5283	19.2750
α_3	1.8809	2.0901
α_4	6.9815	7.8598

3.2.2. Definition of the boundary conditions

Chord end fixity condition in tubular joints of offshore structures ranges from almost fixed to almost pinned with generally being closer to almost fixed (Efthymiou, 1988). In the view of the fact that the effect of the chord end restraints on the stress distribution at the brace/chord intersection is only significant for joints with $\alpha < 8$ and high β and γ values (Smedley and Fisher, 1991; Morgan and Lee, 1998), which do not commonly occur in practice, both chord ends were assumed to be fixed, with the

corresponding nodes restrained. For a joint with the brace member of sufficient length, the brace end fixity imposes marginal effects on the joint strength (Choo et al., 2006). The sufficient brace length is discussed in Sect. 3.3. In the present research, no restraint was applied to the upper end brace members.

3.2.3. Mesh generation and analysis

ANSYS 16 element type SOLID Brick 185 was used to model the chord, braces, and the weld profiles. These elements have compatible displacements and are well-suited to model curved boundaries. The element is defined by eight nodes having three degrees of freedom per node and may have any spatial orientation. Using this type of 3-D brick elements, the weld profile can be modeled as a sharp notch. This method will produce more accurate and detailed stress distribution near the intersection in comparison with a simple shell analysis (See Sect. 3.2.4). To guarantee the mesh quality, a sub-zone mesh generation method was

used during the FE modeling. In this method, the entire structure is divided into several different zones according to the computational requirements. The mesh of each zone is generated separately and then the mesh of entire structure is produced by merging the meshes of all the sub-zones. This method can easily control the mesh quantity and quality and avoid badly distorted elements. The mesh generated by this method for a two-planar DK-joint is shown in Fig. 3. In order to make sure that the results of the FE analysis are not affected by the inadequate quality or the size of the generated mesh, convergence test was conducted and meshes with different densities were used in this test, before generating the 81 models. The static analysis of linearly elastic type is suitable for the prediction of LJF in tubular joints (Gao et al., 2014; Gao and Hu, 2015). The Young's modulus and Poisson's ratio were taken to be 207 GPa and 0.3, respectively.

3.2.4. Validation of the FE model

The accuracy of FE results to determine the f_{LJF} in tubular joints should be validated using the experimental test results. To the best of the authors' knowledge, there is no experimental/FE database of f_{LJF} for two-planar tubular DK-joints currently available in the literature. Considering this issue, in order to verify the FE model used in the present study, a set of Y-joints were modeled and the f_{LJF} values obtained from these models were compared with the experimental results of Fessler et al. (1986), values predicted by Fessler et al. equation (1986), and the FE results of Gao et al. (2014). Geometrical properties of the validating Y-joints have been presented in Table 1. The procedure of geometrical modeling (introducing the chord, braces, and weld profiles), the mesh generation method (including the selection of the element type and size), the analysis type, and the method of f_{LJF} calculation are the same for the validating Y-joint models and the DK-joints used in the present research for the parametric study. Hence, the verification of the f_{LJF} values derived from the validating FE models with available corresponding experiment-/FE-/equation-predicted values lends some support to the validity of the f_{LJF} values derived from the DK-joint FE models.

Results of the FE validation process have been presented in Fig. 4 along with Tables 2 and 3. The effects of the element type and the weld profile were also investigated. A comparison between the results obtained by the solid and shell elements indicated that the solid elements lead to more accurate f_{LJF} values. Moreover, the comparison of solid models with and without the weld profile showed that the omission of the weld profile results in the increase of the error percentage. As can be seen in Fig. 4, there is a good agreement between the results of previous studies and the predictions of the

validating FE model. According to Table 2, the maximum difference between the f_{LJF} of the validating FE model and the experimental results of Fessler et al. (1986) is 10.07%; and Table 3 indicates that the maximum difference between the results of the validating FE model and the equation proposed by Fessler et al. (1986) is 12%. Hence, generated FE models can be considered to be accurate enough to provide valid results.

3.3. Parametric investigation

Using ANSYS, a total of 81 FE models were generated and analyzed in order to study the effects of geometrical parameters on the f_{LJF} in two-planar DK-joints subjected to two types of axial loading (Fig. 1c). Different values assigned to the parameters β , γ , τ , and θ are as follows: $\beta = 0.4, 0.5, 0.6$; $\gamma = 12, 18, 24$; $\tau = 0.4, 0.7, 1.0$; and $\theta = 30^\circ, 45^\circ, 60^\circ$. These values cover the practical ranges of dimensionless parameters typically found in tubular joints of offshore jacket structures. Providing that the gap between the braces is not very large, the relative gap ($\zeta = g / D$) has no considerable effect on the stress and strain distribution. The validity range for this statement is $0.2 \leq \zeta \leq 0.6$ (Lotfollahi-Yaghin and Ahmadi, 2010). Hence, a typical value of $\zeta = 0.3$ was designated for all joints. Sufficiently long chord greater than six chord diameters (i.e. $\alpha \geq 12$) should be used to ensure that the stresses at the brace/chord intersection are not affected by the chord's boundary conditions (Efthymiou, 1988). Hence, in this study, a realistic value of $\alpha = 16$ was designated for all the models. The brace length has no effect on the stress and strain distribution when the parameter α_B is greater than a critical value (Chang and Dover, 1999). According to Chang and Dover (1996), this critical value is about 6. In the present study, in order to avoid the effect of short brace length, a realistic value of $\alpha_B = 8$ was assigned for all joints.

3.4. Organization of the f_{LJF} samples

The f_{LJF} values extracted from the results of 162 FE analyses were organized as two samples for further statistical and probabilistic analyses. Samples 1 and 2 included the f_{LJF} values under the 1st and 2nd axial loading conditions, respectively. Values of the size (n), mean (μ), standard deviation (σ), coefficient of skewness (α_3), and coefficient of kurtosis (α_4) for these samples are listed in Table 4. The value of α_3 for both samples is positive which means that the probability distribution for both samples is expected to have a longer tail on the right, which is toward increasing values, than on the left. Moreover, the value of α_4 for both samples is greater than three meaning that the probability distribution is expected to be sharp-peak (leptokurtic) for both of the prepared samples.

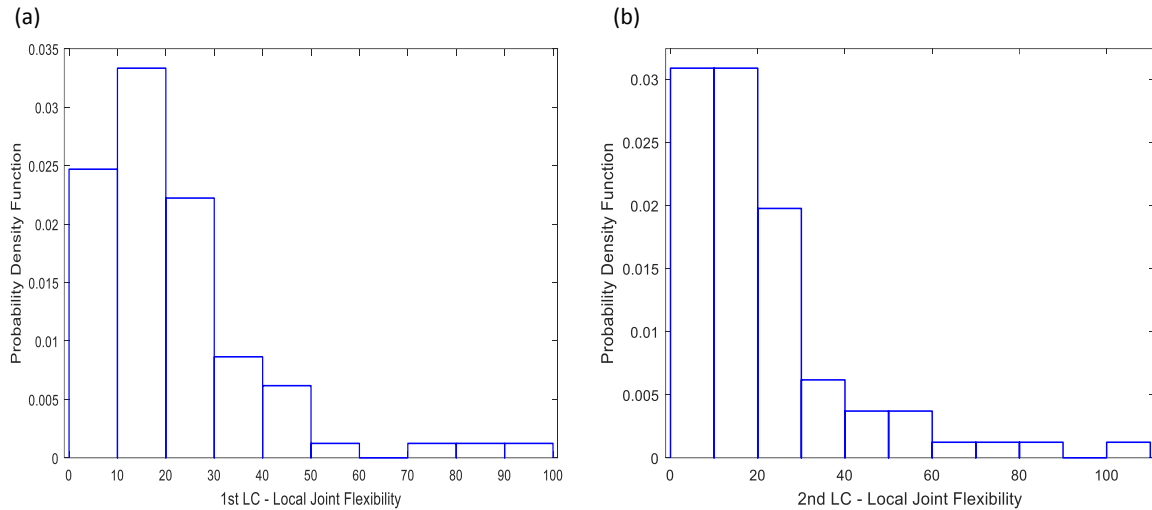


Fig. 5. Density histograms generated for the f_{LJF} samples: (a) Sample 1 (1st axial load case), (b) Sample 2 (2nd axial load case)

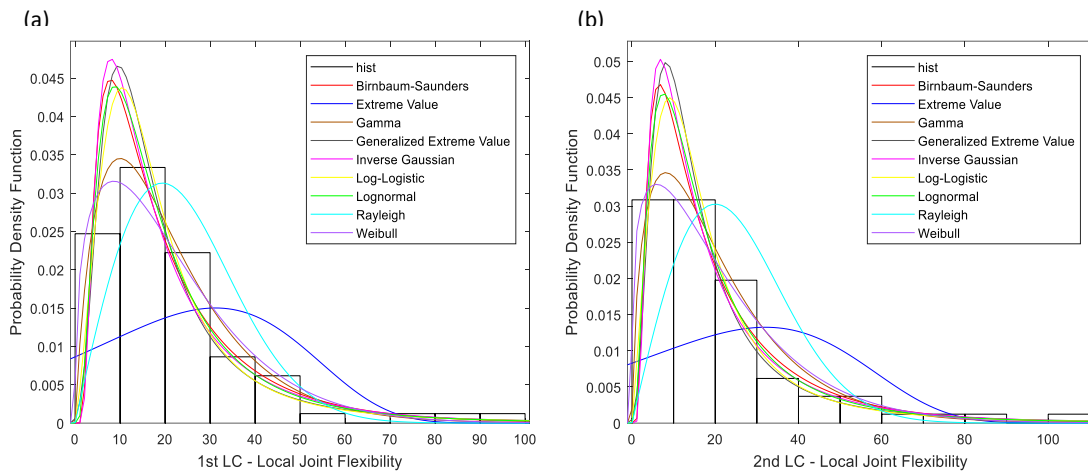


Fig. 6. Probability density functions fitted to the histograms generated for the f_{LJF} : (a) Sample 1 (1st axial load case), (b) Sample 2 (2nd axial load case)

Table 5. Estimated parameters for PDFs fitted to the density histograms of f_{LJF} samples

Fitted PDF	Parameters	Estimated values	
		Sample 1 (1 st axial load case)	Sample 2 (2 nd axial load case)
Birnbaum-Saunders	β_0	15.9317	15.0622
	γ_0	0.810684	0.881752
Extreme Value	μ	31.1966	32.0565
	σ	24.5044	27.7648
Gamma	a	1.89486	1.62996
	b	11.1664	12.8116
Generalized Extreme Value	k	0.383676	0.470146
	σ	8.43034	8.12338
	μ	12.197	11.035
Inverse Gaussian	μ	21.1588	20.8825
	λ	27.6517	22.4881
Log-logistic	μ	2.7632	2.694
	σ	0.441026	0.47553
Lognormal	λ	2.76555	2.70181
	η	0.76643	0.825349
Rayleigh	b	19.3796	20.0377
Weibull	a	23.2737	22.5457
	b	1.35068	1.23608

4. Developing the density histograms based on the Freedman-Diaconis rule

To develop a density histogram, the range of data (R) is divided into a number of classes and the number of occurrences in each class is counted and tabulated. These are called frequencies. Then, the relative frequency of each class can be obtained through dividing its frequency by the sample size. Afterwards, the density is calculated for each class through dividing the relative frequency by the class width. The width of classes is usually made equal to facilitate interpretation.

Care should be exercised in the choice of the number of classes (n_c). Too few will cause an omission of some important features of the data; too many will not give a clear overall picture because there may be high fluctuations in the frequencies. One of the widely accepted rules to determine the number of classes is the Freedman-Diaconis rule expressed as follows (Kottegoda and Rosso, 2008):

$$n_c = \frac{R(n^{1/3})}{2(\text{IQR})} \quad (4)$$

where R is the range of sample data, n is the sample size, and IQR is the interquartile range calculated as:

$$\text{IQR} = Q_3 - Q_1 \quad (5)$$

where Q_1 is the lower quartile which is the median of the lower half of the data; and likewise, Q_3 is the upper quartile that is the median of the upper half of the data.

Density histograms of generated samples are shown in Fig. 5. This figure shows that, as it was expected from the values of α_3 and α_4 in Table 4, the right tail is longer than the left one in both of the histograms. Also, both histograms are leptokurtic.

5. PDF fitting based on the ML method

Nine different PDFs were fitted to the density histograms to assess the degree of fitting of various distributions to the f_{LJF} samples (Fig. 6). In each case, distribution parameters were estimated using the maximum likelihood (ML) method. Results are given in Table 5. The ML procedure is an alternative to the method of moments. As a means of finding an estimator, statisticians often give it preference. For a random variable X with a known PDF, $f_X(x)$, and observed values x_1, x_2, \dots, x_n , in a random sample of size n , the likelihood function of ω , where ω represents the vector of unknown parameters, is defined as:

$$L(\omega) = \prod_{i=1}^n f_X(x_i | \omega) \quad (6)$$

The objective is to maximize $L(\omega)$ for the given data set. It is done by taking m partial derivatives of $L(\omega)$, where m is the number of parameters, and equating them to zero. Then the maximum likelihood estimators (MLEs) of the parameter set ω can be found from the solutions of equations. In this way the greatest probability is given to the observed set of events, provided that the true form of the probability distribution is known.

6. Assessment of the goodness-of-fit

6.1. Kolmogorov-Smirnov test

The Kolmogorov-Smirnov goodness-of-fit test is a nonparametric test that relates to the cumulative distribution function (CDF) of a continuous variable. The test statistic, in a two-sided test, is the maximum absolute difference (which is usually the vertical distance) between the empirical and hypothetical CDFs. For a continuous variate X , let $X^{(1)}, X^{(2)}, \dots, X^{(n)}$ represent the order statistics of a sample of the size n , that is, the values arranged in increasing order. The empirical or sample distribution function $F_n(x)$ is a step function. This gives the proportion of values not exceeding x and is defined as:

$$F_n(x) = \begin{cases} 0, & \text{For } x < x^{(1)} \\ k/n, & \text{For } x^{(k)} \leq x < x^{(k+1)} \quad k = 1, 2, \dots, n-1 \\ 1, & \text{For } x \geq x^{(n)} \end{cases} \quad (7)$$

Empirical distribution functions for generated f_{LJF} samples have been shown in Fig. 7.

Let $F_0(x)$ denote a completely specified theoretical continuous CDF. The null hypothesis H_0 is that the true CDF of X is the same as $F_0(x)$. That is, under the null hypothesis:

$$\lim_{n \rightarrow \infty} \Pr[F_n(x) = F_0(x)] = 1 \quad (8)$$

The test criterion is the maximum absolute difference between $F_n(x)$ and $F_0(x)$, formally defined as:

$$d_n = \sup_x |F_n(x) - F_0(x)| \quad (9)$$

Theoretical continuous CDFs fitted to the empirical distribution functions of generated f_{LJF} samples have been shown in Fig. 8.

A large value of this statistic (d_n) indicates a poor fit. Hence, acceptable values should be known. The critical values $D_{n,\xi}$ for large samples, say $n > 35$, are $(1.3581/\sqrt{n})$ and $(1.6276/\sqrt{n})$ for $\xi = 0.05$ and 0.01 , respectively (Kottegoda and Rosso, 2008) where ξ is the significance level. Results of the Kolmogorov-Smirnov test for the two prepared samples are given in Tables 6 and 7. It is evident in Tables 6 and 7 that the Inverse Gaussian distribution has the smallest d_n value for both samples. Hence, the Inverse Gaussian is the best-fitted distribution for both f_{LJF} samples (Fig. 9).

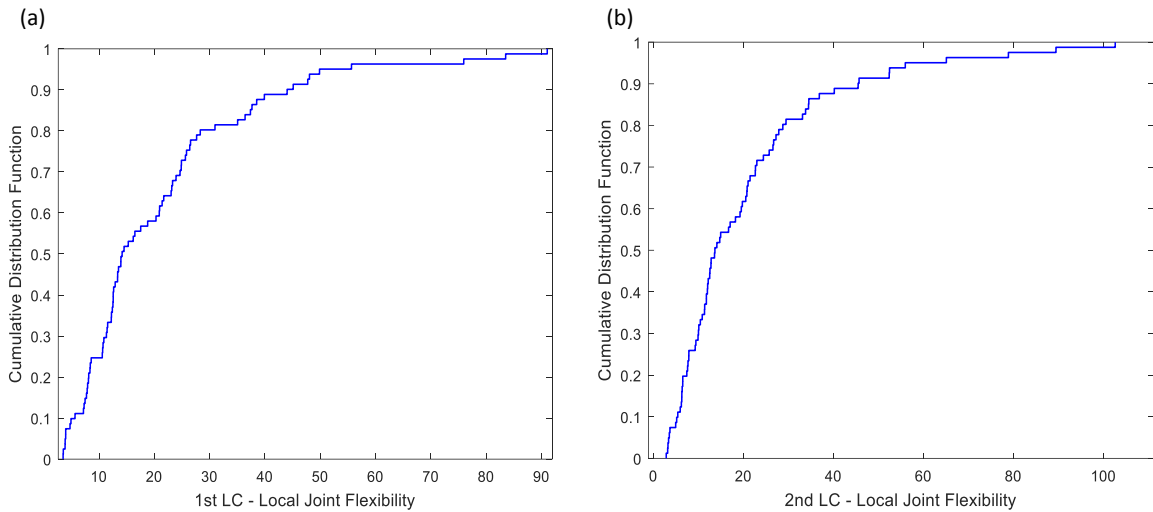


Fig. 7. Empirical cumulative distribution functions for generated f_{LJF} samples: (a) Sample 1 (1st axial load case), (b) Sample 2 (2nd axial load case)

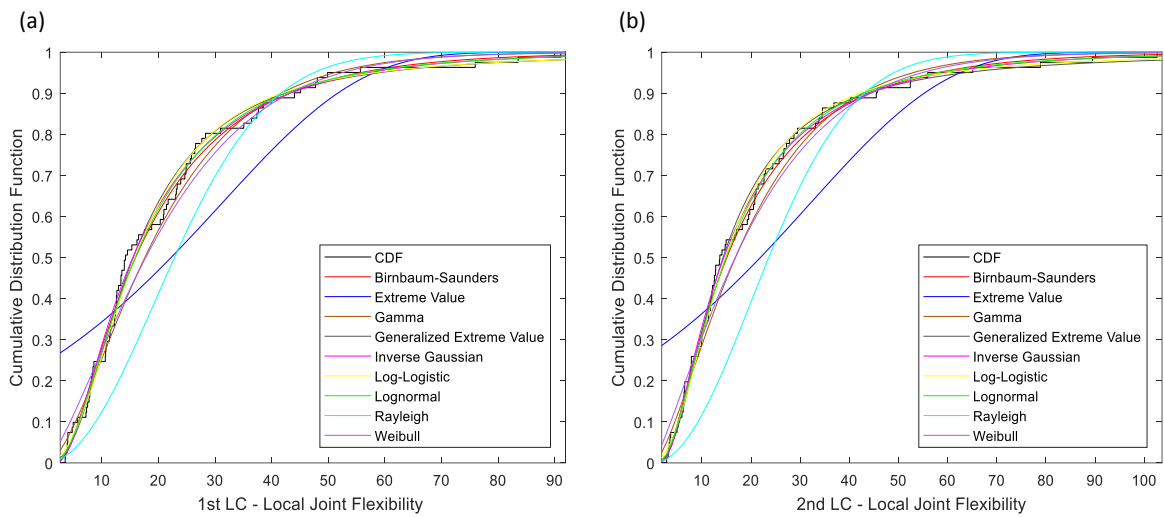


Fig. 8. Theoretical continuous CDFs fitted to the empirical CDFs of generated f_{LJF} samples: (a) Sample 1 (1st axial load case), (b) Sample 2 (2nd axial load case)

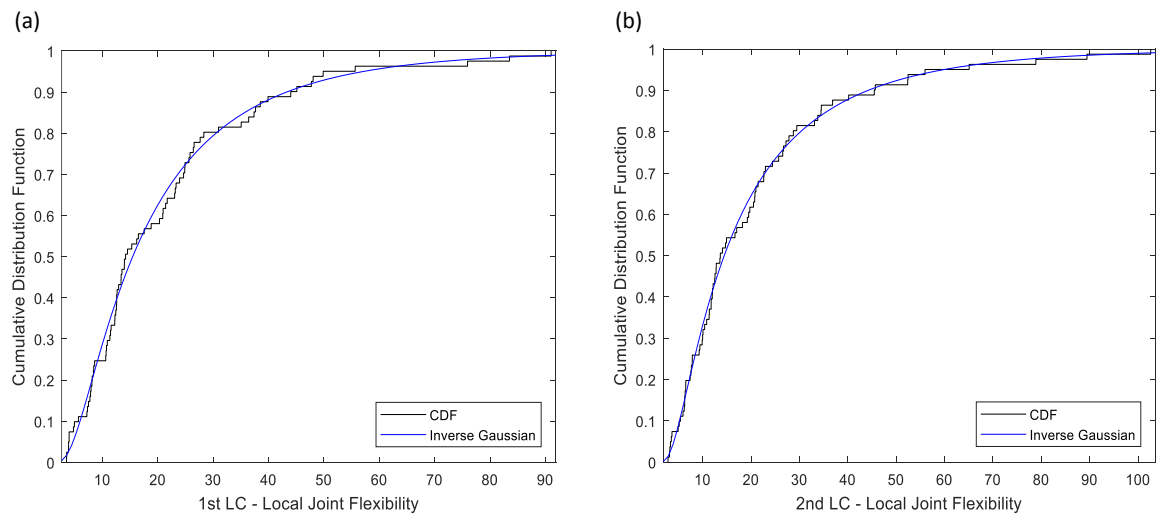


Fig. 9. The best-fitted distribution according to the Kolmogorov-Smirnov test: (a) Sample 1 (1st axial load case), (b) Sample 2 (2nd axial load case)

Table 6. Results of the Kolmogorov-Smirnov goodness-of-fit test for f_{LJF} sample 1 (1st axial load case)

Fitted distribution	Test statistic	Critical value		Test result	
		$\xi=0.05$	$\xi = 0.01$	$\xi=0.05$	$\xi=0.01$
Birnbaum-Saunders	0.063874			Accept	Accept
Extreme Value	0.276059			Reject	Reject
Gamma	0.111909			Accept	Accept
Generalized Extreme Value	0.056169			Accept	Accept
Inverse Gaussian	0.055187	0.1509	0.180844444	Accept	Accept
Log-logistic	0.069035			Accept	Accept
Lognormal	0.065211			Accept	Accept
Rayleigh	0.273597			Reject	Reject
Weibull	0.107671			Accept	Accept

Table 7. Results of the Kolmogorov-Smirnov goodness-of-fit test for f_{LJF} sample 2 (2nd axial load case)

Fitted distribution	Test statistic	Critical value		Test result	
		$\xi=0.05$	$\xi = 0.01$	$\xi=0.05$	$\xi=0.01$
Birnbaum-Saunders	0.054855			Accept	Accept
Extreme Value	0.294516			Reject	Reject
Gamma	0.101506			Accept	Accept
Generalized Extreme Value	0.052595			Accept	Accept
Inverse Gaussian	0.038857	0.1509	0.180844444	Accept	Accept
Log-logistic	0.056989			Accept	Accept
Lognormal	0.054796			Accept	Accept
Rayleigh	0.301174			Reject	Reject
Weibull	0.091919			Accept	Accept

6.2. Chi-squared test

The chi-squared test is a test of significance based on the chi-squared statistic. The statistic is derived by the sum of squares of independent standard normal variates. The main steps are the ranking of a sample of data, division into a number of classes depending on the magnitudes and the range, and the fitting of a probability distribution. The statistic comes from the weighted sum of squared differences between the observed and theoretical frequencies. To test whether the differences between the observed and expected frequencies are significant, following statistic is used:

$$X^2 = \sum_{i=1}^{n_c} \frac{(O_i - E_i)^2}{E_i} \tag{10}$$

The observed frequencies O_i are found by multiplying the relative frequencies, for each class i from a total of n_c classes, by the sample size n . The expected frequencies E_i are the products of the total sample size n and the areas under the PDF, as specified by the null hypothesis, between the bounds of each class i .

A large value of the test statistic indicates a poor fit; so the acceptable values should be known. The critical value is $\chi_{1-\xi, \nu}^2$ where $\nu = n_c - k - 1$ represents the degrees of freedom and k is the number of parameters estimated from the same data used for the test. $\chi_{1-\xi, \nu}^2$ is the value which a chi-squared variate X exceeds with probability ξ , i.e.:

$$\Pr[X \leq \chi_{1-\xi, \nu}^2] = \int_0^{\chi_{1-\xi, \nu}^2} f_X(x) dx = 1 - \xi \tag{11}$$

$$f_X(x) = \begin{cases} \frac{1}{2^{\nu/2} \Gamma(\nu/2)} x^{(\nu-2)/2} e^{-x/2} & x \geq 0 \\ 0 & x < 0 \end{cases} \tag{12}$$

$$\Gamma(\nu/2) = \int_0^\infty x^{(\nu/2)-1} e^{-x} dx \tag{13}$$

The number of classes was determined based on (4). Results of chi-squared test for the two prepared samples are given in Tables 8 and 9. It is evident in Tables 8 and 9 that the Log-logistic and Generalized Extreme Value distributions have the smallest values of the test statistic for Samples 1 and 2, respectively. Hence, based on the chi-squared test, these are the best-fitted distributions for the generated samples (Fig. 10).

7. Proposed probability distribution model for the f_{LJF}

The best fitted distributions for the generated f_{LJF} samples were introduced in Sect. 6. It was indicated that according to the results of the Kolmogorov-Smirnov test, the Inverse Gaussian distribution is the best probability model for both f_{LJF} samples; while according to the chi-squared test, the Log-logistic and Generalized Extreme Value distributions are the best probability models for Samples 1 and 2, respectively.

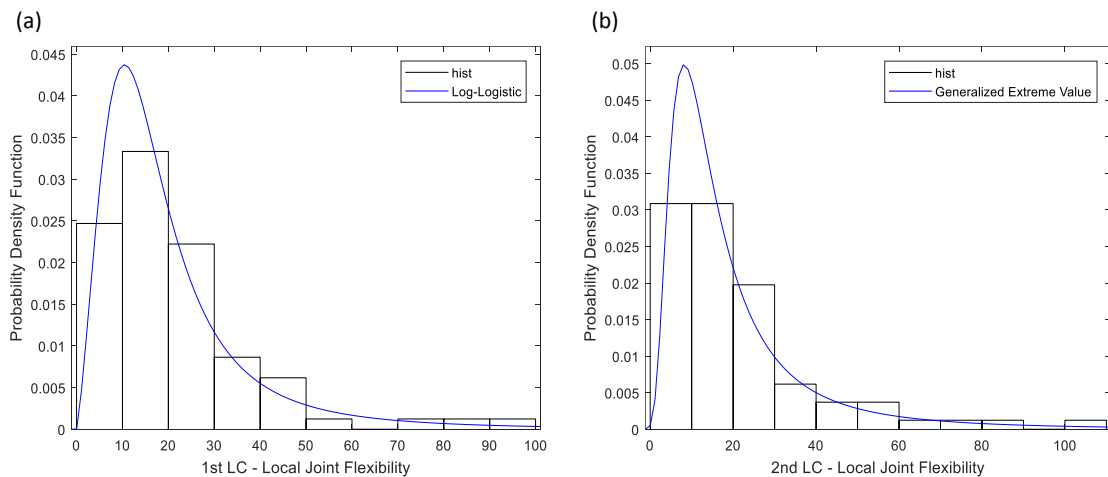
It can be seen that the best-fitted distributions for the two studied samples according to the Kolmogorov-Smirnov and chi-squared tests include three different models: Inverse Gaussian, Log-logistic, and Generalized Extreme Value distributions.

Table 8. Results of the chi-squared goodness-of-fit test for f_{LJF} sample 1 (1st axial load case)

Fitted distribution	Test statistic	Critical value		Test result	
		$\xi = 0.05$	$\xi = 0.01$	$\xi=0.05$	$\xi=0.01$
Birnbaum-Saunders	6.495821	14.06714045	18.47530691	Accept	Accept
Extreme Value	832.9629			Reject	Reject
Gamma	13.11403			Accept	Accept
Generalized Extreme Value	5.913662			Accept	Accept
Inverse Gaussian	6.233059			Accept	Accept
Log-logistic	5.652407			Accept	Accept
Lognormal	5.713852			Accept	Accept
Rayleigh	727.3675			Reject	Reject
Weibull	15.03414			Reject	Accept

Table 9. Results of the chi-squared goodness-of-fit test for f_{LJF} sample 2 (2nd axial load case)

Fitted distribution	Test statistic	Critical value		Test result	
		$\xi = 0.05$	$\xi = 0.01$	$\xi=0.05$	$\xi=0.01$
Birnbaum-Saunders	5.943618	15.50731306	20.09023503	Accept	Accept
Extreme Value	1378.228			Reject	Reject
Gamma	15.95741			Reject	Accept
Generalized Extreme Value	5.024573			Accept	Accept
Inverse Gaussian	5.035435			Accept	Accept
Log-logistic	5.240546			Accept	Accept
Lognormal	5.173702			Accept	Accept
Rayleigh	3489.074			Reject	Reject
Weibull	15.12464			Accept	Accept

**Fig. 10.** The best-fitted distributions according to the chi-squared test: (a) Sample 1 (1st axial load case), (b) Sample 2 (2nd axial load case)

The diversity of the best-fitted probability models derived for the studied f_{LJF} values may practically result in the confusion and difficulty of their application for the reliability-based analysis and design. Hence, reducing the number of distribution types proposed for the f_{LJF} values might be a good idea. In order to do so, the top three distribution functions for each f_{LJF} sample were identified (Tables 10 and 11). The aim was to propose a single probability model to cover both f_{LJF} samples. It should be noted that, for each sample, all of the three mentioned functions have acceptable fit according to the Kolmogorov-Smirnov and chi-squared tests (Tables 6-9).

After surveying the data presented in Tables 10 and 11, the Inverse Gaussian model is proposed as the governing probability distribution function for the f_{LJF} values. The difference between the test statistics of the proposed distribution and the best-fitted one for each sample is presented in Tables 12

and 13. Using the information presented in these tables, the analyst is able to make a choice, based on the engineering judgment, between the best-fitted and the proposed probability models for each of the four studied load cases.

The PDF of the Inverse Gaussian distribution is expressed as:

$$f_X(x) = \sqrt{\frac{\lambda}{2\pi x^3}} \exp\left\{-\frac{\lambda}{2\mu^2 x}(x - \mu)^2\right\} \quad (14)$$

After substituting the values of estimated parameters from Table 5, following probability density functions are proposed for the f_{LJF} values in two-planar tubular DK-joints subjected to the two considered axial load cases defined in Fig. 1c:

1st axial load case:

$$f_X(x) = \sqrt{\frac{4.4009}{x^3}} \exp\left\{-\frac{0.0309}{x}(x - 21.1588)^2\right\} \quad (15)$$

Table 10. Best-fitted distributions for the f_{LJF} samples based on the results of the Kolmogorov-Smirnov test

Best-fitted distributions	f_{LJF} samples	
	Sample 1 (1 st axial load case)	Sample 2 (2 nd axial load case)
# 1	Inverse Gaussian	Inverse Gaussian
# 2	Generalized Extreme Value	Generalized Extreme Value
# 3	Birnbaum-Saunders	Lognormal

Table 11. Best-fitted distributions for the f_{LJF} samples based on the results of the chi-squared test

Best-fitted distributions	f_{LJF} samples	
	Sample 1 (1 st axial load case)	Sample 2 (2 nd axial load case)
# 1	Log-logistic	Generalized Extreme Value
# 2	Lognormal	Inverse Gaussian
# 3	Generalized Extreme Value	Lognormal

Table 12. Comparison of the test statistics for the proposed and the best-fitted distributions based on the results of the Kolmogorov-Smirnov test

	Test statistic	
	Sample 1 (1 st axial load case)	Sample 2 (2 nd axial load case)
Best-fitted distribution	0.055187 (Inverse Gaussian)	0.038857 (Inverse Gaussian)
Proposed distribution	0.055187 (Inverse Gaussian)	0.038857 (Inverse Gaussian)
Difference	0%	0%

Table 13. Comparison of the test statistics for the proposed and the best-fitted distributions based on the results of the chi-squared test

	Test statistic	
	Sample 1 (1 st axial load case)	Sample 2 (2 nd axial load case)
Best-fitted distribution	5.652407 (Log-logistic)	5.024573 (Generalized Extreme Value)
Proposed distribution	6.233059 (Inverse Gaussian)	5.035435 (Inverse Gaussian)
Difference	10.27%	0.22%

2nd axial load case:

$$f_X(x) = \sqrt{\frac{3.5791}{x^3}} \exp\left\{-\frac{0.0258}{x}(x - 20.8825)^2\right\} \quad (16)$$

where X denotes the f_{LJF} as a random variable and x represents its values.

Suggested PDFs can be adapted in the reliability-based analysis and design of axially loaded two-planar tubular DK-joints commonly used in offshore jacket-type wind turbines and oil/gas production platforms.

8. Conclusions

A total of 162 FE analyses were carried out on 81 FE models of two-planar tubular DK-joints subjected to two types of axial load cases. Generated FE models were validated using the available experimental data, FE results, and design formulas. FE analysis results were used to develop a set of PDFs for the f_{LJF} in axially loaded DK-joints. Based on a parametric FE investigation, two samples were created for the f_{LJF} and density histograms were

generated for these samples. Nine theoretical PDFs were fitted to the developed histograms and the ML method was applied to evaluate the parameters of fitted PDFs. In each case, the Kolmogorov-Smirnov and chi-squared tests were used to assess the goodness of fit. Finally, the Inverse Gaussian model was suggested as the governing probability distribution function for the f_{LJF} . After substituting the values of estimated parameters, two fully defined PDFs were presented for the f_{LJF} in two-planar tubular DK-joints under two types of axial loading.

Acknowledgments

The assistance from Mr. Ali Ziaei Nejad during the numerical analysis is highly appreciated. Useful comments of anonymous reviewers on draft version of the paper are also highly appreciated.

References

- Ahmadi H, Lotfollahi-Yaghin MA, "A probability distribution model for stress concentration factors in multi-planar tubular DKT-joints of steel offshore structures", *Applied Ocean Research*, 2012, 34, 21-32.
- Ahmadi H, Lotfollahi-Yaghin MA, "Geometrically parametric study of central brace SCFs in offshore three-planar tubular KT-joints", *Journal of Constructional Steel Research*, 2012, 71, 149-161.
- Ahmadi H, Lotfollahi-Yaghin MA, Aminfar MH, "Effect of stress concentration factors on the structural integrity assessment of multi-planar offshore tubular DKT-joints based on the fracture mechanics fatigue reliability approach", *Ocean Engineering* 2011, 38, 1883-1893.
- Ahmadi H, Lotfollahi-Yaghin MA, Aminfar MH, "Geometrical effect on SCF distribution in uni-planar tubular DKT-joints under axial loads", *Journal of Constructional Steel Research*, 2011, 67 (8), 1282-1291.
- Ahmadi H, Lotfollahi-Yaghin MA, Shao YB, Aminfar MH, "Parametric study and formulation of outer-brace geometric stress concentration factors in internally ring-stiffened tubular KT-joints of offshore structures", *Applied Ocean Research*, 2012, 38, 74-91.
- Ahmadi H, Mayeli V, "Probabilistic analysis of the local joint flexibility in two-planar tubular DK-joints of offshore jacket structures under in-plane bending loads", *Applied Ocean Research*, 2018, 81 (12), 126-140.
- Ahmadi H, Mayeli V, "Development of a probability distribution model for the LjF factors in offshore two-planar tubular DK-joints subjected to OPB moment loading", *Marine Structures*, 2019, 63 (1), 196-214.
- Ahmadi H, Mayeli V, Zavvar E, "A Probability distribution model for the degree of bending in tubular KT-joints of offshore jacket-type platforms subjected to IPB moment loadings", *International Journal of Coastal and Offshore Engineering*, 2019, 3 (2), 11-29.
- Ahmadi H, Zavvar E, "The effect of multi-planarity on the SCFs in offshore tubular KT-joints subjected to in-plane and out-of-plane bending loads", *Thin-Walled Structures*, 2016, 106, 148-165.
- Ahmadi H, Ziaei Nejad A, "Local joint flexibility of two-planar tubular DK-joints in OWTs subjected to axial loading: Parametric study of geometrical effects and design formulation", *Ocean Engineering* 2017, 136 (5), 1-10.
- Ahmadi H, Ziaei Nejad A, "A study on the local joint flexibility (LjF) of two-planar tubular DK-joints in jacket structures under in-plane bending loads", *Applied Ocean Research*, 2017, 64 (3), 1-14.
- Ahmadi H, Ziaei Nejad A, "Geometrical effects on the local joint flexibility of two-planar tubular DK-joints in jacket substructure of offshore wind turbines under OPB loading", *Thin-Walled Structures*, 2017, 114 (5), 122-133.
- American Welding Society (AWS), "Structural welding code: AWS D 1.1.", Miami (FL): American Welding Society, US, 2002.
- Bouwkamp JG, Hollings JP, Masion BF, Row DG, "Effect of joint flexibility on the response of offshore structures", *Offshore Technology Conference (OTC)*, Houston, Texas, 1980, 455-464.
- Buitrago J, Healy BE, Chang TY, "Local joint flexibility of tubular joints", *International Conference on Ocean, Offshore & Arctic Engineering (OMAE)*, Glasgow, UK, 1993, 405-417.
- Chang E, Dover WD, "Parametric equations to predict stress distributions along the intersection of tubular X and DT-joints", *International Journal of Fatigue* 1999, 21, 619-635.
- Chang E, Dover WD, "Stress concentration factor parametric equations for tubular X and DT joints", *International Journal of Fatigue*, 1996, 18 (6), 363-387.
- Chen B, Hu Y, Tan M, "Local joint flexibility of tubular joints of offshore structures", *Marine Structures* 1990, 3, 177-197.
- Chen B, Hu Y, Xu H, "Theoretical and experimental study on the local flexibility of tubular joints and its effect on the structural analysis of offshore platforms", *Proceedings of the 5th International Symposium on Tubular Structures*, Nottingham, UK; 1993, 543-550.
- Chen TY, Zhang HY, "Stress analysis of spatial frames with consideration of local flexibility of multiplanar tubular joint", *Engineering Structures*, 1996, 18 (6), 465-471.
- Choo YS, Qian XD, Wardenier J, "Effects of boundary conditions and chord stresses on static strength of thick-walled CHS K-joints", *Journal of Constructional Steel Research*, 2006, 62, 316-328.
- Det Norske Veritas, "Rules for the design, construction and inspection of offshore structures", Norway, 1977.
- Efthymiou M, "Development of SCF formulae and generalized influence functions for use in fatigue analysis", *Offshore Tubular Joints (OTJ)* 88, Surrey, UK, 1988.
- Efthymiou M, "Local rotational stiffness of un-stiffened tubular joints", *RKER report*; 1985, 185-199.
- Fessler H, Mockford PB, Webster JJ, "Parametric equations for the flexibility matrices of single brace tubular joints in offshore structures", *Proceedings of the Institution of Civil Engineers* 1986, 81, 659-673.
- Fessler H, Mockford PB, Webster JJ, "Parametric equations for the flexibility matrices of multi-brace tubular joints in offshore structures", *Proceedings of the Institution of Civil Engineers*, 1986, 81, 675-696.
- Gao F, Hu B, "Local joint flexibility of completely overlapped tubular joints under out-of-plane bending", *Journal of Constructional Steel Research*, 2015, 115, 121-130.
- Gao F, Hu B, Zhu HP, "Local joint flexibility of completely overlapped tubular joints under in-plane bending", *Journal of Constructional Steel Research*, 2014, 99, 1-9.
- Gao F, Hu B, Zhu HP, "Parametric equations to predict LjF of completely overlapped tubular joints under lap brace axial loading", *Journal of Constructional Steel Research*, 2013, 89, 284-292.
- Golafshani AA, Kia M, Alanjari P, "Local joint flexibility element for offshore platforms structures", *Marine Structures*, 2013, 33, 56-70.
- Hoshiyari I, Kohoutek R, "Rotational and axial flexibility of tubular T-joints", *Proceedings of the 3rd International Offshore and Polar Engineering Conference (ISOPE)*, Singapore, 1993, 192-198.
- Hu Y, Chen B, Ma J, "An equivalent element representing local flexibility of tubular joints in structural analysis of offshore platforms", *Computers & Structures*, 1993, 47 (6), 957-969.

- Karamanos SA, Romeijn A, Wardenier J, "Stress concentrations in multi-planar welded CHS XX-connections", *Journal of Constructional Steel Research*, 1999, 50, 259-282.
- Kottegoda NT, Rosso R, "Applied statistics for civil and environmental engineers", 2nd Edition, Blackwell Publishing Ltd, UK, 2008.
- Lotfollahi-Yaghin MA, Ahmadi H, "Effect of geometrical parameters on SCF distribution along the weld toe of tubular KT-joints under balanced axial loads", *International Journal of Fatigue*, 2010, 32, 703-719.
- Morgan MR, Lee MMK, "Prediction of stress concentrations and degrees of bending in axially loaded tubular K-joints", *Journal of Constructional Steel Research*, 1998, 45 (1), 67-97.
- Nassiraei H, "Static strength of tubular T/Y-joints reinforced with collar plates at fire induced elevated temperature", *Marine Structures*, 2019, 67, 102635.
- Nassiraei H, Lotfollahi-Yaghin MA, Ahmadi H, "Static performance of doubler plate reinforced tubular T/Y-joints subjected to brace tension", *Thin-Walled Structures* 2016, 108, 138-152.
- Nassiraei H, Lotfollahi-Yaghin MA, Neshaei SA, Zhu L, "Structural behavior of tubular X-joints strengthened with collar plate under axially compressive load at elevated temperatures", *Marine Structures*, 2018, 61, 46-61.
- Nassiraei H, Mojtahedi A, Lotfollahi-Yaghin MA, Zhu L, "Capacity of tubular X-joints reinforced with collar plates under tensile brace loading at elevated temperatures", *Thin-Walled Structures*, 2019, 142, 426-443.
- Nassiraei H, Lotfollahi-Yaghin MA, Ahmadi H, Zhu L, "Static strength of doubler plate reinforced tubular T/Y-joints under in-plane bending load", *Journal of Constructional Steel Research*, 2017, 136, 49-64.
- Smedley P, Fisher P, "Stress concentration factors for simple tubular joints", *Proceedings of the International Offshore and Polar Engineering Conference (ISOPE)*, Edinburgh, UK, 1991.
- Ueda Y, Rashed SMH, Nakacho K, "An improved joint model and equations for flexibility of tubular joints", *Offshore Mechanics and Arctic Engineering*, 1990, 112, 157-168.
- Underwater Engineering Group, "Design of tubular joint for offshore structures", UEG/CIRIA, London, UK, 1985.